

A joint theoretical and experimental study of phenylene-acetylene molecular wires

R. J. Magyar and S. Tretiak*

*Theoretical Division and Center for Nonlinear Studies,
Los Alamos National Laboratory, Los Alamos, NM 87545*

Y. Gao, H.-L. Wang and A. P. Shreve

Bioscience Division, Los Alamos National Laboratory, Los Alamos, NM 87545

(Dated: December 3, 2021)

Abstract

The excited state electronic structure of π conjugated phenylene-acetylene oligomers is calculated using time-dependent density functional theory (TD-DFT) approaches. The theoretical fluorescence spectra are analyzed in terms of Frank-Condon active nuclear normal modes and shown to compare well with experiment. Theoretical and experimental results for the optical absorption and emission spectra of these molecules indicate that the conjugation length can be significantly reduced by conformational rotations about the triple-bonded carbon links. This has serious implications on the electronic functionalities of polyphenylene-acetylene based molecular wires and their possible use as charge/energy conduits in nano-assemblies.

PACS numbers: 82.35.Cd, 71.20.Rv, 42.70.Jk

*Electronic address: serg@cnls.lanl.gov

I. INTRODUCTION

In nature, complex nano-assemblies of functional units combine to perform required complicated tasks. One example is the assembly for harvesting light in photosynthesis [1, 2]. There is considerable practical interest in imitating and manipulating this sort of functionality on a nano-scale. In order to do so, theoretical and experimental understanding of the constituents is required. In this paper, we consider a functional component of a possible light harvesting assembly. One functional unit of a light harvesting assembly might be a self-assembled multilayer with the specific function of transferring holes away from light receptors. Conjugated polymers may be good candidates for this purpose because of their semiconductor-like properties, plasticity, and potential low cost of fabrication [3]. These materials have already found uses in a wide range of applications such as light-emitting diodes, lasers, sensors and molecular switches [4, 5, 6, 7].

To perform such functions, the molecule should be rigid in one dimension to provide required spatial conduits. Moreover, the hole-electron separation and charge conduction processes require long conjugation lengths and flexible excited state structure to provide sufficient freedom to tune energetics synthetically. We consider oligomers of phenylene-acetylene, shown on the top panel of Fig. 1, which retain one-dimensional rigidity like molecular wires. However, this polymer can be easily twisted between benzene rings about the triple-bonded carbon links. This geometry change is expected to reduce the conjugation length and may adversely affect applications which rely on the de-localization of the charge carriers. In this article we examine phenylene-acetylene oligomers from both theoretical and experimental standpoints in order to analyze their excited state electronic structure and the effects of conformational rotations on effective conjugation and electronic de-localization lengths of these materials. In particular, we utilized the natural transition orbital decomposition [8] to infer the extent of the underlying electronic localization.

To calculate electronic structure we use a blend of quantum chemical methods including semi-empirical (Austin Model 1 (AM1)) approaches [9] for ground and excited state [10] geometry optimizations, and time-dependent density functional theory (TD-DFT) [11, 12] and ZINDO [13] methods for excited state computations. There have been many theoretical calculations on conjugated polymers using various semi-empirical and first principle approaches. It is well understood that, in general, both semi-empirical (such as AM1) and

DFT methods provide reasonable geometries and ZINDO can deliver good UV-visible spectra for such molecular systems [14, 15]. Even more accurate TD-DFT approaches are able to tackle complicated electronic features such as exciton binding energy [16, 17, 18] and double excitations [19]. Furthermore, based on the results of the calculations, absorption and emission spectra can be modeled, for example, for polyenes, oligoarylenes, phenylenevinyls, and polyfluorenes [10, 20, 21]. Existing theoretical studies of phenylene-acetylene include TD-DFT investigation of the excited states of the monomer [22, 23] and several studies of dendrimer with phenylene-acetylene being the basic unit [24, 25]. Additionally, experimental absorption and fluorescence spectra have been reported for phenylene-acetylene monomers, dimers, and trimers linked to Pt centers [26].

Details of our computational approach are presented in Section II. In Section III we analyze computational results and compare them to experiment. Finally, we discuss the trends that emerge and summarize our findings in Section IV.

II. COMPUTATIONAL METHODOLOGY

We focus on oligomers of two to ten phenylene-acetylene repeat-units (top panel of Fig. 1). The two unit case is the small molecule limit and may be compared to more expensive *ab initio* calculations which are only possible for small systems. In such small molecules photo-excitations are confined by molecular ends and study of increasingly longer chains is necessary to understand the onset of de-localized excitations that polymers exhibit. The ten unit chain is a sufficiently long oligomer to reasonably approximate the infinite polymer limit [14, 15].

Ground state optimal geometries of phenylene-acetylene oligomers have been obtained using the Gaussian 98 [27] software package. The molecular geometries in the gas phase are fully optimized using the semi-empirical AM1 method. The AM1 model has been parametrized to give accurate geometries for organic molecules and is expected to provide reliable geometries [9]. To model the fluorescence spectra, the excited state geometries are needed. We used the excited-state molecular dynamics (ESMD) computational package [10] to optimize molecular geometries for the lowest excited state at time-dependent Hartree-Fock (TD-HF) level and AM1 model. This approach allows treatment of large molecular systems at modest numerical cost and previously resulted in reasonable fluorescence line-shapes of

several conjugated molecular systems [10, 21]. In principle, it is also possible to use DFT or Hartree-Fock *ab initio* approaches for ground state optimization purposes. However, such approaches may be problematic for the excited state optimization due to high numerical cost. Instead, we treat molecular geometries within the same approach: HF/AM1 and TD-HF/AM1 levels for the ground and excited states, respectively. Additionally, by using the AM1, we eliminate any errors in the geometry that might come from using approximate functionals and limited basis sets in density functional theory. For example, it was found for polyacetylene that a fraction of exact-exchange must be mixed with a semi-local exchange-correlation functional for the theory to reproduce the bond-length alternation accurately [28].

For obtained geometries, we next calculate the excited-state triplet and singlet manifolds using TD-DFT approach which is known to be a reliable but computationally affordable *ab initio* tool for excited state treatment. We perform all our calculations in the gas phase for simplicity, but we expect that the results will not change much when these oligomers are placed in non-polar solvents. We use the B3LYP functional combined with the 6-31G basis set as implemented in the Gaussian 98 package [27]. The 6-31G basis set is known to be an efficient blend of accuracy and manageable size for large conjugated molecules [29]. We do not include diffuse functions as we expect the relevant excited states have support only along the backbone of the polymer for long chains. For ground-state properties, DFT provides a formally exact scheme for solving the many-body problem [30], but, in practice, the functionals used are approximated in a manner convenient for calculations. The B3LYP functional [31] combines semi-local exchange-correlation with non-local exact-exchange. By construction, this functional handles a fraction of long-range exchange exactly but fails to capture long-range correlation effects. Time-dependent density functional theory is an extension of density functional theory in which many-body excitations are associated with the poles of the exact density response [11, 12]. TD-DFT using B3LYP inputs has been shown to be accurate for many molecular systems and is computationally affordable. In particular, Ref. [32] suggests that B3LYP is the optimal functional to use for excited-state calculations on PPV-type polymers.

In order to characterize calculated excited states and to address the electronic localization, we performed a transition orbital analysis [8] based on the computed transition densities from the TD-DFT calculations. This analysis offers the most compact representa-

tion of a given transition density in terms of its expansion in single-particle transitions. The transition orbital picture provides an important information on the multi-configurational nature of a given excited state, and gives a real-space orbital representation as to where the photo-excited hole and electron reside, which is useful to illustrate the excitonic localization phenomena.

Finally, we calculate the line-shapes of fluorescence spectra using the ground and excited state optimal geometries and vibrational normal modes of the ground state. This can be readily done within the Condon approximation for displaced multidimensional harmonic oscillators [20, 33]. The vibrational overlap integrals $|\langle 0|\nu_n\rangle|^2 = \frac{e^{-S_n} S_n^\nu}{\nu!}$, Franck-Condon factors, govern the probability of emission from transition between the vibrational level 0 in the lowest excited state and a vibrational level n in the ground state. These quantities, in turn, depend on the dimensionless displacements Δ_n of each normal mode with Huang-Rhys factors, $S_n = \Delta_n^2/2$. The fluorescence band shape as a function of the frequency ω is determined by the imaginary part of the polarizability [20, 33]

$$\alpha(\omega) = \text{Im} \left\{ \mu^2 \sum_{\nu_1} \cdots \sum_{\nu_{3N-6}} \frac{\prod_{n=1}^{3N-6} \langle 0|\nu_n\rangle^2}{\Omega^{(0)} - \sum_{n=1}^{3N-6} \nu_n \omega_n - \omega - i\Gamma} \right\}, \quad (1)$$

where μ is the electronic transition dipole moment between the excited and the ground-state, $\Omega^{(0)}$ is the associated 0 – 0 transition energy, the ω_n 's are the vibrational frequencies, the ν_n 's are the quanta of the participating normal modes, and Γ is an empirical parameter setting the spectral line-widths. We choose the line-width to be either 0.2 eV or 0.02 eV. The former produces plots which agree well with the experimentally observed line widths, whereas the latter allows greater resolution and the analysis in terms of the contributing vibrational states.

III. RESULTS AND DISCUSSIONS

The chemical structure of phenylene-acetylene is shown on Fig. (1). Our specimen is terminated at one end by a methyl group (CH_3) and at the other end by an amine group (NH_2) which may either be used for binding the molecule to to a substrate or for self-assembly into structures of interest at the air-water interface (Langmuir-Blodgett method). Oligomers with $N=2,3$, and 4 repeat units have been synthesized and spectroscopically characterized. The phenylene-acetylene oligomers were synthesized by cross-coupling of the

appropriate phenylacetylene compounds with 4-amino-1-iodobenzene using $Pd(PPh_3)_4/CuI$ as catalyst. The molecular building block (Phenylene-acetylene) is prepared by coupling 4-dodecane-ethynylbenzene with 4-(trimethylsilylethynyl) iodobenzene. The solution UV-vis and fluorescence spectra were measured using methylene chloride as the solvent.

We calculate the threshold for rotation about the triple bond is ~ 0.05 eV per triple bond, and we expect that at room temperature where $k_B T \approx 0.025$ eV, an ensemble of geometries will be allowed given the uncertainty of solvent effects and molecular packing. In order to estimate how these geometry changes will affect the spectrum, we sample two extreme geometries (Fig. 1), the completely planar configuration where all benzene rings lie in the same plane, and an alternating configuration where adjacent benzene rings are at right angles to each other. Both geometries are local minima within the AM1 approach, the planar case being the global minimum. Even though in total ground-state energies the two configurations do not differ drastically, their excited-states properties do. Torsional potentials for another type of conjugated polymer have been calculated in detail [34]. Here we choose only to calculate the extreme limits and some intermediates arguing that the general behavior and trends will be thereby evident and the details of the torsional potential are not critical to the current study.

In Fig 1, we plot the dependence of the energy of the uv-visible active singlet state as a function of chain length for absorption and fluorescence. Absorption results are presented for a planar, a completely alternating, and an intermediate geometry where every other benzene is rotated about the triple bond by 45 degrees. The experimental results are the absorption and fluorescence maxima in a non-polar solvent, methylene chloride. Except for in the alternating geometry, the lowest S_1 state has the largest oscillator strength. We see that the experiment lies between the intermediate and completely alternating results. The long chain limit is reached by approximately four to six repeat units for planar chain, which implies the extent of the conjugation length and the size of the photo-generated exciton. This value is a strong function of the exact orbital-dependent exchange (Fock-like exchange) present in the functional [35]. For example, the ZINDO (100% of exact-exchange) curve saturates faster to the constant long-chain-limit than B3LYP (20% of exact-exchange) results. Since the alternating geometry breaks some of the conjugation, we observe several low-lying dark singlets energetically below the optically active *band-gap* state. In this case, the energy of the *band-gap* state has little size-dependence and is significantly blue-shifted compared to

that for planar geometry. As expected, the intermediate geometry values lie between these two extremes and are accidentally very close to the ZINDO results. In order to estimate the effective bond angle (within TD-B3LYP/6-31G approach), we gradually rotated the benzene rings about the triple bonds and calculated the singlet excited states for $N=2, 3,$ and 4 unit oligomers. For most angles, the lowest singlet state can be directly associated with the lowest singlet state for the planar geometry. At some critical angle, this breaks down and the lowest singlet is no longer optically active. For 2-units, the singlet and experiment do not overlap for any angle. For 3-units, the overlap is at 43 degrees. The effective rotation angle for 4-unit chains is over 63 degrees. In the long chain limit, we expect the effective angle to increase but saturate.

Geometric effects are important for fluorescence as well. Here the excited state geometries remain close to planar with a steep torsional potential as has been reported for other polymers [10, 21]. The bond-length alternation parameter reduces in the middle of the molecule which indicates an excitonic self-trapping process. Because of the tendency of the excited state to planarize the molecule, the alternating geometry is unlikely, so we simulate what one might expect to become of the alternating geometry by taking the relaxed excited state geometry and rotating each benzene by 45 degrees about the triple bond while leaving two to three benzene rings in the center of the chain coplanar. We see that the fluorescence from the simulated alternating geometry differs only slightly from the planar geometry (pointing to the short extent of the self-trapped exciton). The curve for the simulated case is not smooth because of the scheme we use to simulate the geometry. For even numbered chains we have two coplanar benzenes in the center of the chain, but for odd numbered chains, we have three coplanar benzenes and a slightly greater de-localization. Therefore, the results for the first excited singlets of odd chain lengths are systematically slightly lower.

Using Eq. (1) it is possible to compare the experimental and theoretical fluorescence spectra directly (see Fig. 2). The top panel shows the experimental absorption spectra for 2-4 unit chains. The next panel is the experimental emission spectra. As expected, experimental absorption-fluorescence spectra are nearly mirror-image profiles; this indicates the same nature of the absorbing and emitting electronic state. The last two panels are theoretical results calculated with broadening parameters of 0.2 eV and 0.02 eV, respectively. The larger broadening is able to model experimentally measured line shapes. Indeed we observe good overall comparison between theory and experiment. In particular, the shoulder on the

red-side of all spectra are well reproduced. The $\Gamma = 0.02$ eV broadening gives spectra which show more detail than experiment and offer the possibility of identification and analysis of the dominant vibrational modes. In the theoretical absorption plots, three peaks can easily be resolved. They correspond, from left to right, to a 0-0 transition, a benzene bond alternating mode, and a fast triple bond length oscillation. In the ten unit chain, we can also resolve a peak from an alternate benzene bond mode. Figure 3 shows schematically the dominant normal modes of phenylene-acetylene . The top shows the low-frequency stretching mode I of the entire molecule, which contribute for the most part to the width of vibronic peaks. Its frequency and displacement Δ depends on the molecular mass. These quantities decrease and increase for large oligomers, respectively. The other three nuclear modes (II-IV) coupled to the electronic system are high-energy vibrations whose frequencies weakly depend on the chain length. The first two (II and III) are bond alternating modes within the benzene rings that only become resolved for the longer chain lengths. The last mode IV is the stretching of the triple-bond. Relative displacements are shown for the individual modes. The left value is for the shortest chain and the right is for the ten unit chain. We see that the higher energy modes become less dominant as the polymer’s length is increased. The strength of the low energy stretching mode nearly doubles in the long chain limit relative to the short chain limit, and the sub-dominant alternating modes such as the second benzene alternating mode become resolved in the longer chain length limit.

Figure 4 shows the size-scaling of calculated low-lying excited states as a function of reciprocal conjugation length. The top panel displays a typical structure of singlet and triplet manifolds in conjugated polymers where the ladder of well-defined states is optically coupled. Nearly linear scaling for all states allows extrapolation to the saturated values in the infinite chain limit. As expected, the singlet-excitation energies (S_1) become lower with increasing polymer length. The long-chain limit is achieved approximately (within 0.2 eV) by six units. The optically inactive first triplet excited state (T_1) has been calculated using two levels of theory: the TD-DFT approach for the lowest triplet excitation and change in the self-consistent field (Δ SCF) method. The latter is the energy difference between the self-consistent ground states calculated with enforced singlet and triplet spin multiplicities. We observe negligible spin contamination in the unrestricted approach used to calculate the triplet ground state. In general, Δ SCF is considered to be a stable and reliable approach for evaluating the first triplet state energy. In contrast, TD-DFT energies of triplet states

strongly depend on the amount of the HF exchange present in the functional. Even negative energies of triplet states may be observed in the TD-HF limit (so-called triplet instability). In our case (B3LYP functional) we found 2 and 2.4 eV saturation limits for the energy of the T_1 state of phenylene-acetylene in TD-DFT and Δ SCF approaches, respectively. Higher lying T_n and S_n states correspond to de-localized excitations where the electron become well separated from the hole upon absorption of a quantum of light [14]. Even though the spin state matters for small molecules, T_n and S_n correctly become degenerate in the long chain limit, saturating to 2.8 eV limit. In the alternating geometry case, the electron is expected to remain localized. All excitations for the alternating geometry are about 0.5 eV greater than for the planar geometry because of the more local nature of the excitation.

In order to characterize the typical low-lying (T_1 and S_1) excitations we further performed a transition orbital analysis [8]. The top of Fig. 5 shows the transition orbitals for 2, 4, and 10 unit chains of planar phenylene-acetylene . As expected, all these states represent de-localized transitions which are mostly $\pi - \pi^*$ nature. Note that for the longest (ten unit) chains, the triplets are more localized than the singlets. For the singlet state, one pair of orbitals dominates. Both the hole and particle are de-localized along the backbone of the polymer; however, the hole is more de-localized. Triplet states adopt more of a multi-configurational character with increasing chain length, which reflects their smaller exciton size compared to that of singlet states. The bottom of Fig. 5 displays the transition orbitals for the alternating geometry. These plots clearly show the breakage of conjugation due to torsion. All excitations have multi-configurational character as a superposition of orbitals with an electron-hole pair residing on short chain segments (e.g., see T_1 for N=10). Ultimately such excitations in long chains can be well treated in the Frenkel exciton limit.

IV. CONCLUSION

The extent of electronic de-localization and the existence of appropriate excited state energetics have serious implications for using conjugated polymers as a constituent in artificial functional nano-assemblies. Our study confirms that torsional disorder of the molecular geometry caused by dielectric environment or thermal fluctuation is an important factor affecting the excited state structure of phenylene-acetylene . We find that DFT can give quantitatively accurate results when compared to experiment. Subsequently, the nature

of calculated electronic states can be analyzed in the real-space using a transition orbital decomposition. The good agreement between the experimental and theoretical fluorescence spectral line-shapes indicate that we can use theory to understand the underlying molecular morphology and to identify and analyze Franck-Condon active vibrational modes. By comparing our theoretical calculations to the experimental results, we find an effective average geometry and argue that the conjugation length is drastically reduced by rotations about the triple-bonds.

Section III contains only a fraction of the results we obtained using combination of different methods. Overall, we observe two fundamental trends: I) The bond-length alternation parameter reduces with decreasing a fraction of exact Fock-like exchange in the DFT functional in the course of the ground state geometry optimization. This results in the overall red-shift of the excitation energies. II) An increase of a fraction of exact exchange in the functional when computing TD-DFT excited states results in the blue (red) shift of singlet (triplet) state energies. Consequently, any combination of physically justified methods and appropriate model chemistries will result in the same trends and conclusions with some variation of calculated spectroscopic variables.

Acknowledgments

The research at LANL is supported by Center for Nonlinear Studies (CNLS), the LANL LDRD program, and the office of Science of the US Department of Energy. This support is gratefully acknowledged.

-
- [1] T. Pullerits and V. Sundström, *Acc. Chem. Res.* **29**, 381 (1996).
 - [2] V. Sundström, T. Pullerits, and R. van Grondelle, *J. Phys. Chem. B* **103**, 2327 (1999).
 - [3] R. H. Friend *et al.*, *Nature* **397**, 121 (1999).
 - [4] C. Schmitz, P. Posch, M. Thelakkat, H. W. Schmidt, A. Montali, K. Feldman, P. Smith, and C. Weder, *Adv Func. Mat.* **11**, 41 (2001).
 - [5] F. Hide, M. A. Diaz-Garcia, B. J. Schwartz, M. R. Andersson, Q. B. Pei, and A. J. Heeger, *Science* **273**, 1833 (1996).
 - [6] J. S. Yang and T. M. Swager, *J. Am. Chem. Soc.* **120**, 5321 (1998).

- [7] A. R. Brown, A. Pomp, C. M. Hart, and D. M. Deleeuw, *Science* **270**, 972 (1995).
- [8] R. L. Martin, *J. Chem. Phys.* **118**, 4775 (2003).
- [9] M. J. S. Dewar, E. G. Zoebisch, E. F. Healy, and J. J. P. Stewart, *J. Am. Chem. Soc.* **107**, 3902 (1985).
- [10] S. Tretiak, A. Saxena, R. L. Martin, and A. R. Bishop, *Phys. Rev. Lett.* **89**, 097402 (2002).
- [11] E. Runge and E. K. U. Gross, *Phys. Rev. Lett.* **52**, 997 (1984).
- [12] M. E. Casida, in *Recent Advances in Density-Functional Methods*, Vol. 3 of *Part I*, edited by D. A. Chong (World Scientific, Singapore, 1995).
- [13] J. Ridley and M. C. Zerner, *Theor. Chim. Acta* **32**, 111 (1973).
- [14] J. L. Brédas, J. Cornil, D. Beljonne, D. A. dos Santos, and Z. Shuai, *Acc. Chem. Res.* **32**, 267 (1999).
- [15] S. Tretiak and S. Mukamel, *Chem. Rev.* **102**, 3171 (2002).
- [16] A. Ruini, M. J. Caldas, G. Bussi, and E. Molinari, *Phys. Rev. Lett.* **88**, 206403 (2002).
- [17] J. W. van der Horst, P. A. Bobbert, M. A. J. Michels, G. Brocks, and P. J. Kelly, *Phys. Rev. Lett.* **83**, 4413 (1999).
- [18] M. Rohlfing and S. G. Louie, *Phys. Rev. Lett.* **82**, 1959 (1999).
- [19] N. T. Maitra, K. Burke, and C. Woodward, *Phys. Rev. Lett.* **89**, 023002 (2002).
- [20] S. Karabunarliev, M. Baumgarten, E. Bittner, and K. Mullen, *J. Chem. Phys.* **113**, 11372 (2000).
- [21] I. Franco and S. Tretiak, *Chem. Phys. Lett.* **372**, 403 (2003).
- [22] L. Serrano-Andres, M. Merchan, and M. Jablonski, *J. Chem. Phys.* **119**, 4294 (2003).
- [23] Y. Amatatsu and Y. Hasebe, *J. Phys. Chem. A* **107**, 11169 (2003).
- [24] A. L. Thompson, K. M. Gaab, J. J. Xu, C. J. Bardeen, and T. J. Martinez, *J. Phys. Chem. A* **108**, 671 (2004).
- [25] S. Tretiak, V. Chernyak, and S. Mukamel, *J. Phys. Chem. B* **102**, 3310 (1998).
- [26] D. G. McLean, J. E. Rogers, and T. M. Cooper, *Proc. SPIE - Int. Soc. Opt. Eng.* **4462**, 11 (2002).
- [27] M. J. Frisch *et al.*, *Gaussian 98 (Revision A.11)* (Gaussian, Inc., Pittsburgh PA, 2002).
- [28] C. H. Choi, M. Kertesz, and A. Karpfen, *J. Chem. Phys.* **107**, 6712 (1997).
- [29] A. M. Masunov and S. Tretiak, *J. Phys. Chem. B* **108**, 899 (2004).
- [30] P. Hohenberg and W. Kohn, *Phys. Rev.* **136**, 864 (1964).

- [31] A. D. Becke, *J. Chem. Phys.* **98**, 1372 (1993).
- [32] J. S. K. Yu, W. C. Chen, and C. H. Yu, *J. Phys. Chem. A* **107**, 4268 (2003).
- [33] A. B. Myers, R. A. Mathies, D. J. Tannor, and E. J. Heller, *J. Chem. Phys.* **77**, 3857 (1982).
- [34] A. Karpfen, C. H. Choi, and M. Kertesz, *J. Phys. Chem. A* **101**, 7426 (1997).
- [35] S. Tretiak, K. Igumenshchev, and V. Chernyak, Exciton sizes of conducting polymers predicted by a time-dependent density functional theory, *Phys. Rev. B*, 2004, (in press).

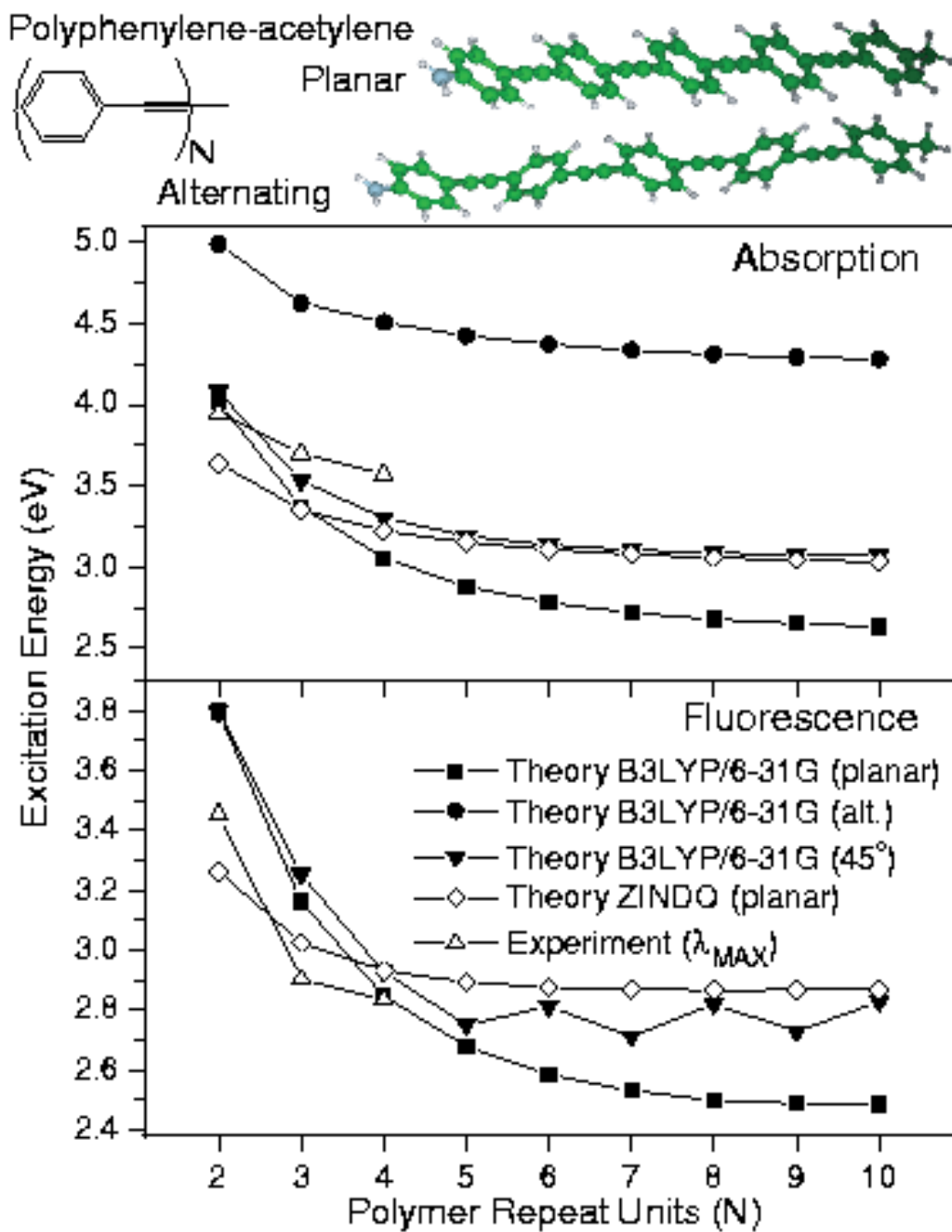


FIG. 1: Top: molecular structure of phenylene-acetylene and schematic structures of the planar and alternating geometries respectively. Middle: scaling of the energy of the singlet excited state which dominates uv-visible absorption as a function of the number of polymer repeat units. Theoretical values correspond to the vertical excitation and emission, and experimental values are taken for the absorption and emission maxima. Bottom: Same as above but for fluorescence.

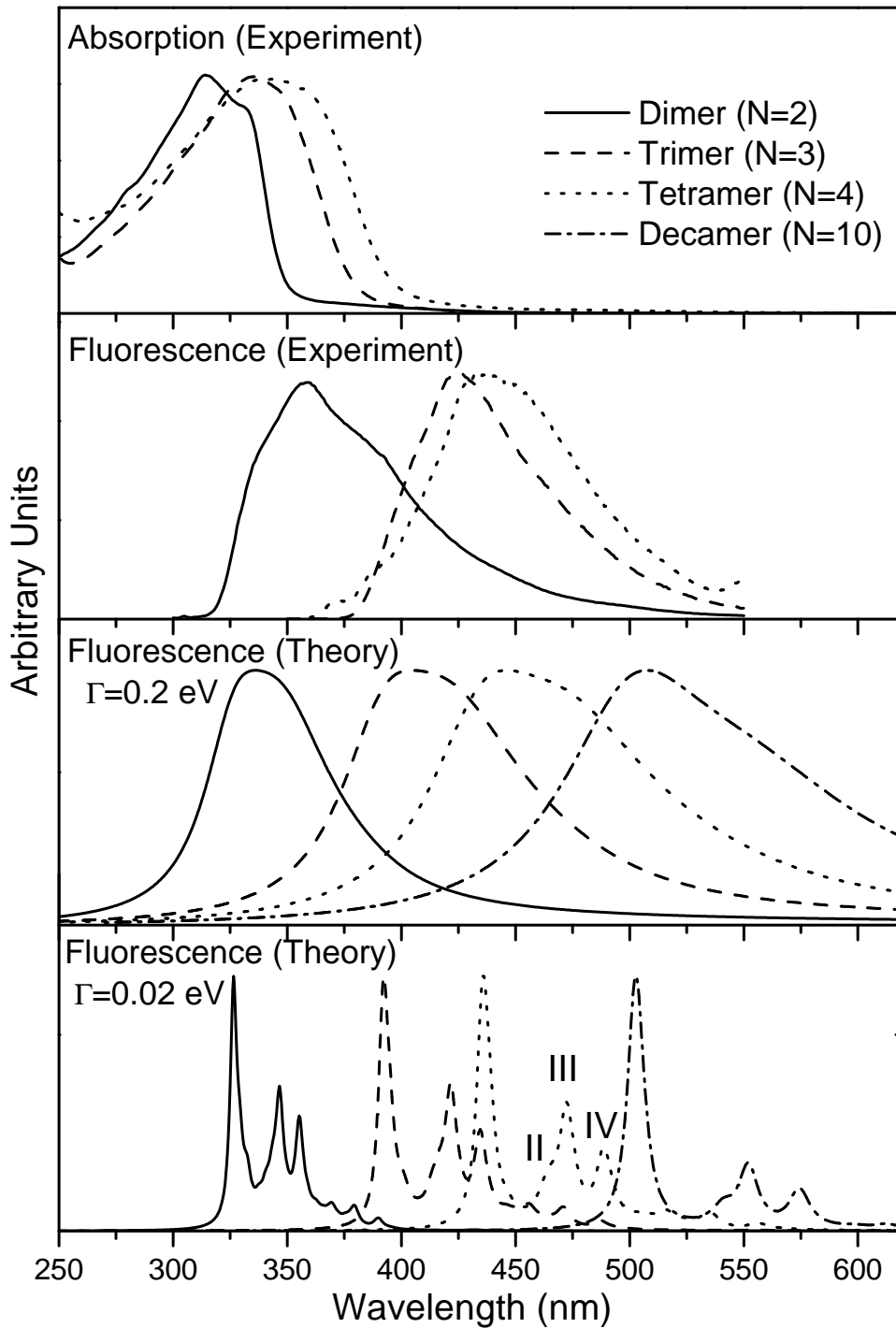


FIG. 2: Absorption and fluorescence line shapes for various length phenylene-acetylene oligomers; experiment versus theory. The top two panels are the experimental absorption and fluorescence. The bottom two panels are the theoretical emission profiles calculated with broad (0.2 eV) and narrow (0.02 eV) spectral line width. Frank-Condon active vibrational normal modes (II-IV) are shown in Fig. 3.

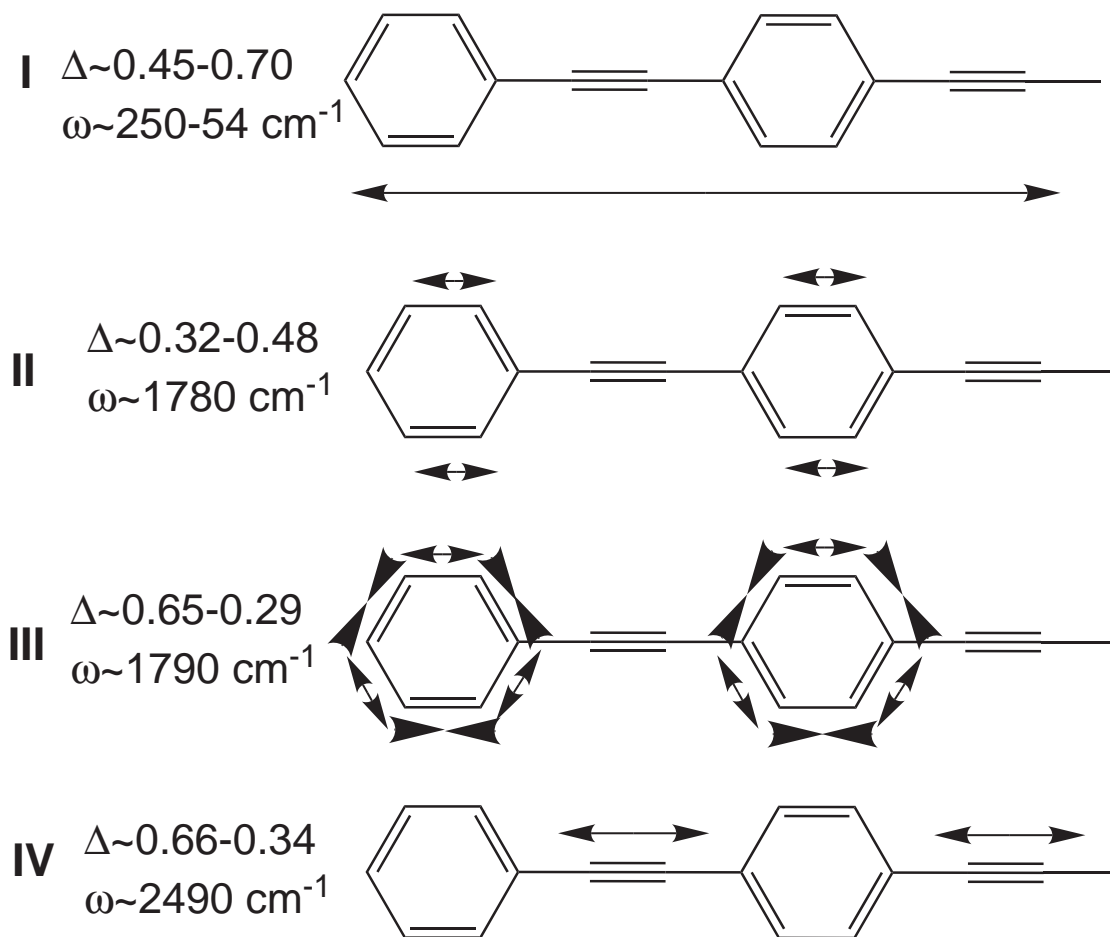


FIG. 3: The dominant normal modes contributing to the vibrational structure of the fluorescence spectrum for phenylene-acetylene. The top diagram is a low energy stretching mode contributing to the spectral broadening. The next two diagrams show vibrations contributing to the II-III peak, which becomes resolved as the polymer length increases; these are oscillations in the length of the bonds within the benzene rings. The final mode is a high energy oscillation in the length of the triple bond, which contributes to the IV peak.

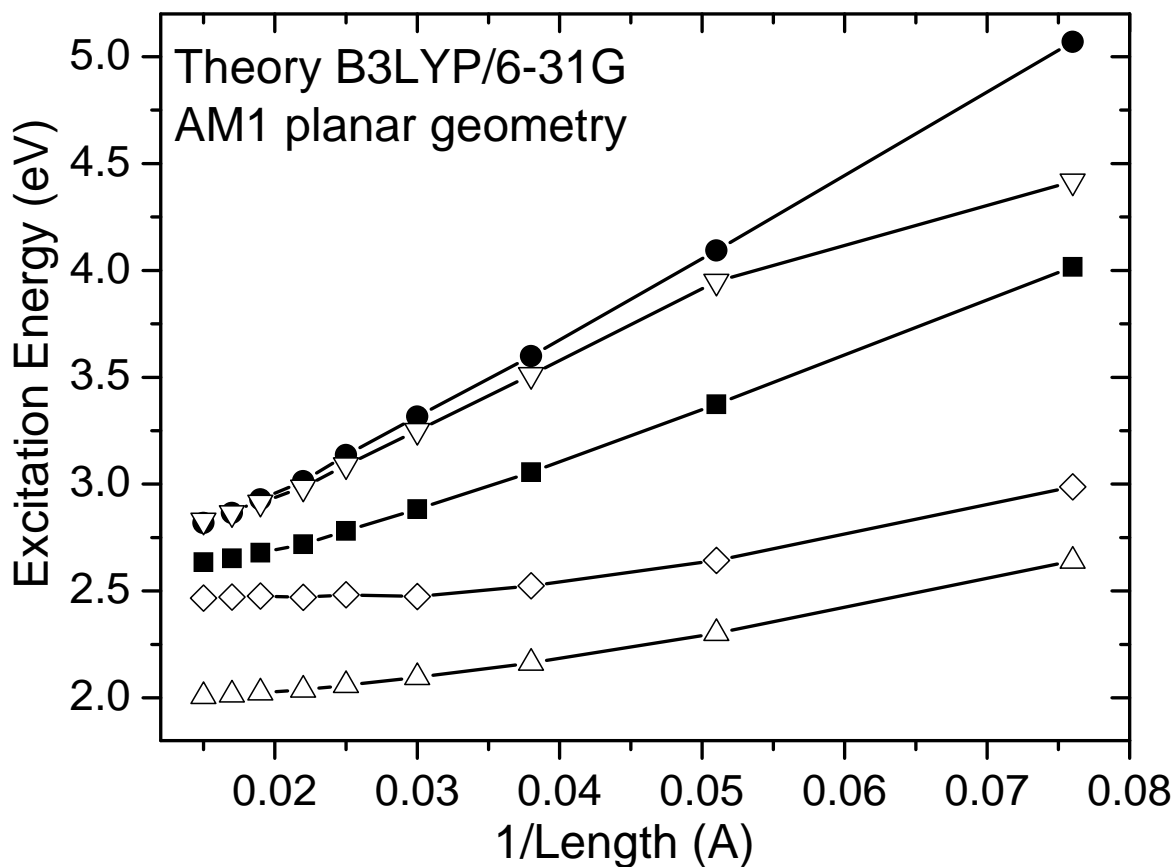
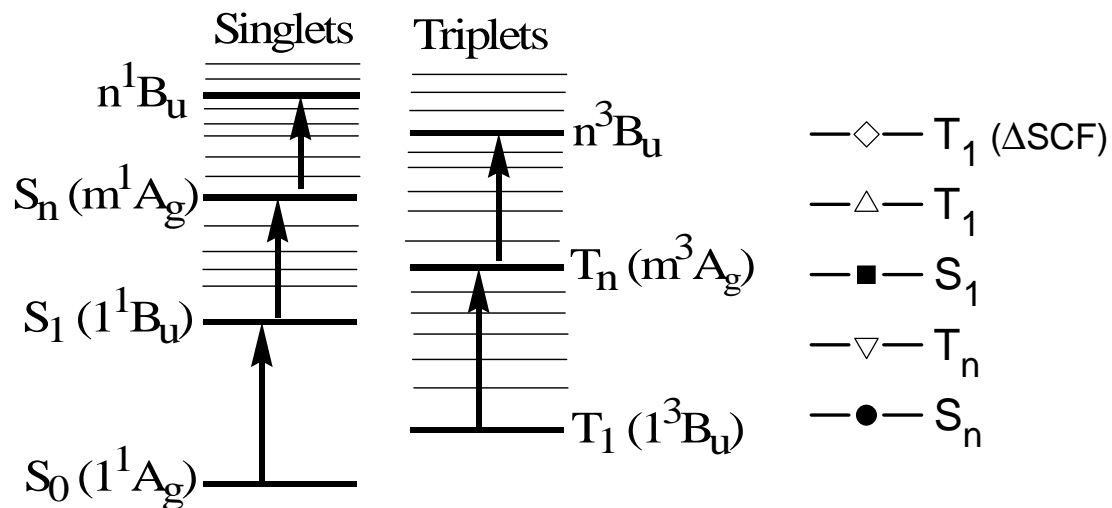


FIG. 4: Top: Typical electronic structure of optically active states in singlet and triplet manifolds for conjugated polymers. Bottom: Size-scaling of excitation energies as a function of the reciprocal conjugation length for phenylene-acetylene oligomers.

	Planar	Alternating
Phenylene-acetylene (2-unit)		
Fig. 2		
T ₁ 10.17eV		
H ₁ 10.17eV		
Phenylene-acetylene (4-unit)		
Fig. 3		
T ₁ 10.14eV		
H ₁ 10.13eV		
Phenylene-acetylene (10-unit)		
Fig. 4		
T ₁ 10.17eV		
H ₁ 10.15eV		
Phenylene-acetylene (2-unit)		
Fig. 5		
T ₁ 10.17eV		
H ₁ 10.15eV		
Phenylene-acetylene (4-unit)		
Fig. 6		
T ₁ 10.19eV		
H ₁ 10.17eV		
Phenylene-acetylene (10-unit)		
Fig. 7		
T ₁ 10.17eV		
H ₁ 10.15eV		
H ₂ 10.16eV		
H ₃ 10.16eV		
H ₄ 10.16eV		
H ₅ 10.16eV		
H ₆ 10.16eV		
H ₇ 10.16eV		
H ₈ 10.16eV		
H ₉ 10.16eV		
H ₁₀ 10.16eV		

FIG. 5: Selected transition orbitals for 2, 4, and 10-unit phenylene-acetylene chains in the planar and alternating ground-state geometries. These are calculated at the B3LYP/6-31G level. The NH₂ end is to the right.